

# Cavity-modified spontaneous-emission rates in liquid microdroplets

H-B. Lin, J. D. Eversole,\* C. D. Merritt, and A. J. Campillo

*Naval Research Laboratory, Laser Physics Branch, Washington, D.C. 20375*

(Received 9 December 1991)

We observe significant lifetime modification (both reduction and lengthening) of 610–620-nm light spontaneously emitted by chelated europium ions in 10- $\mu$ m-diam dimethylformamide-alcohol solution droplets. The enhancement or inhibition of the Einstein  $A$  coefficient over the familiar free-space value is direct evidence of cavity quantum-electrodynamic effects taking place in microdroplets.

PACS number(s): 42.50.Wm, 12.20.Fv, 32.80.-t, 42.55.-f

Cavity quantum electrodynamics (QED) considers the effects of electromagnetic boundary conditions on atomic radiative properties. When atoms are placed in a microcavity, for example, fluorescence may be alternatively enhanced [1–3] or inhibited [4,5] depending on whether or not the emission spectrally coincides with a cavity resonance. This effect was first discussed by Purcell [1], who noted that on resonance the changes in the final density of states per unit volume and unit frequency would lead to a greatly enhanced probability for spontaneous emission over that normally observed in free space. Purcell's formula for the magnitude of the enhancement (i.e., the ratio of cavity-modified  $A$  coefficient to the free-space  $A$  coefficient, here referred to as  $\eta$ ) is given by  $\eta \approx 3DQ\lambda^3/4\pi^2V_m$ . Here  $D$  is the mode degeneracy of the cavity,  $Q$  is the quality factor, and  $V_m$  is the mode volume. Much of the previous experimental work on cavity enhancement at visible wavelengths was performed using Fabry-Pérot cavities [6–8]. A spherical cavity represents a case of three-dimensional enclosure and is attractive because all fields and modes, both internal to and external to the cavity, are exactly calculable in practice. The transverse dependence, consisting of spherical harmonics, allows calculations with one-dimensional simplicity [9]. By contrast, the outwardly simple one-dimensional Fabry Pérot cavity is much more difficult to treat as a realistic quantum-mechanical description requires an unwieldy three-dimensional Cartesian field-dependent calculation. It has been known for some time that nearly transparent microdroplets act as high- $Q$  resonators; the feedback is provided by light waves that totally internally reflect at the droplet-air interface and fold back on themselves [10]. Spherical cavity resonances, often called morphology dependent resonances (MDR's) [10], occur at numerous discrete wavelengths throughout the visible in micrometer sized droplets. For a given droplet, resonances occur at specific values of  $x_{n,l}$ . Here  $x$  is the size parameter given by  $2\pi a/\lambda$ , where  $a$  is the droplet radius, and  $n$  and  $l$  are integers. The mode number  $n$  indicates the order of the spherical Bessel and Hankel functions describing the radial field distribution and the order  $l$  indicates the number of maxima in the radial dependence of the internal field distribution. Both discrete transverse electric and transverse magnetic resonances exist. Emission from dielectric microspheres [11]

and fibers [12] containing fluorescing dyes show sharp line structure superimposed on the normal broadband emission. These spectral features result from cavity QED enhancement of the emission rate at specific spherical cavity resonance wavelengths. Theoretical works [9,13,14] predict large ( $>1500$  times) cavity QED enhancements in the  $A$  coefficient of molecules embedded in such micrometer sized droplets. Recently, significant cavity QED enhanced lasing gain was reported in liquid microdroplets [15]. In the present work, we qualitatively illustrate these effects in droplets by demonstrating both direct lifetime shortening (enhancement) of fluorescence MDR features on resonance and lifetime lengthening (inhibition) off resonance.

Figure 1 outlines the experimental approach. An excited-state population of chelated-europium ions is created just below the droplet surface by pumping an optical resonance [16,17] of the particle with an excitation laser. The resonant mode occupies a volume very near the droplet-air interface; order one modes lie within a micrometer of the surface while higher-order modes extend asymptotically to an inner radius of  $a/m$ , where  $m$  is the index of refraction. Since the predicted emission rate is strongly dependent on radial position [13], excitation at an input resonance emphasizes the cavity behavior of the droplet over its free-space tendencies. The central core region of the droplet displays a lifetime which is very nearly the free-space value (slightly inhibited). When the droplet is uniformly excited, the emission consists of an admixture of modified and free-space emission with radiation from the central region tending to skew the total emission towards free-space characteristics. When an excited-state population is spatially prepared as shown at the top of Fig. 1, the spectral dependence of the  $\text{Eu}^{3+}$  emission will resemble that schematically shown in the middle of Fig. 1. The familiar free-space spectrum will be modified by the addition of one or more peaks at wavelengths corresponding to spherical cavity resonances. At these wavelengths, the emission rate is enhanced (origin of the peaks). The emission rate is a strong function of the radial position, undergoing oscillations [13] especially in the nominal pumped region (Fig. 1, shaded area). Consequently, the decay at any particular wavelength is not a simple exponential. The broad spectral background resembling the usual free-space spectrum schematically

illustrated in the middle of Fig. 1 mostly originates from wavelengths and spatial locations within the pumped region that are inhibited. Therefore, when the spectrum is monitored as a function of time, the MDR peaks should decay more quickly (see bottom of Fig. 1) than the inhibited off-resonance components.

The size of the droplet relative to the spectral bandwidth of the fluorophore is critical to whether or not lifetime changes occur. Purcell's formula assumes weak coupling necessary for application of the golden rule [9]; i.e.,  $\tau_C < \tau_F$ , where  $\tau_C$  and  $\tau_F$  are the cavity and fluorophore lifetimes, respectively. In the Fourier transform limit,

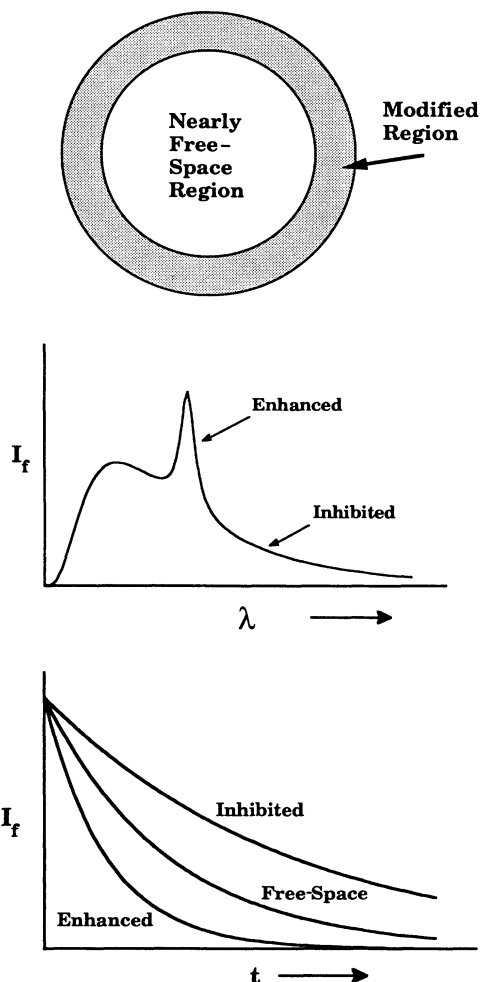


FIG. 1. Outline of the experimental approach. When the droplet is in optical resonance with the exciting laser, an excited-state europium ion population is created near the droplet-air interface (top, shaded region). Within this region, emission rates are modified and spectra appear as illustrated in the middle of the figure. The broad off-resonant spectral components resemble the free-space spectrum, but emanate from inhibited spatial locales and decay more slowly (see bottom). The resonant emission rate is enhanced, leading to the formation of a spectral peak which decays more rapidly than the usual free-space rate. The emission from the droplet rim is an admixture of components displaying both inhibited and enhanced lifetimes.

this may be restated as  $\delta\nu_{HB} < \delta\nu_{MDR}$ , where  $\delta\nu_{HB}$  and  $\delta\nu_{MDR}$  are the spectral widths of the emission (homogeneously broadened) and cavity modes, respectively. When the weak-coupling lifetime condition is met but the emission bandwidth is not Fourier transform limited, a more general expression for the spontaneous-emission rate enhancement is given [18] by

$$\eta = \int_0^\infty \rho_c(\nu) R(\nu) d\nu / \int_0^\infty \rho_b(\nu) R(\nu) d\nu,$$

where  $\rho_c(\nu)$  and  $\rho_b(\nu)$  are the final-state mode density for photons with and without a cavity and  $R(\nu)$  is the volume integrated spontaneous transition rate per mode. In the limit  $\delta\nu_{HB} \ll \delta\nu_{MDR}$ , integration yields Purcell's formula. An important spectral parameter of droplets is  $\Delta\nu_{MDR}$ , the spectral spacing between modes of the same order. This quantity is inversely proportional to droplet radius and approximated [19] by

$$\{\arctan[(m^2 - 1)^{1/2}]\} / 2\pi a (m^2 - 1)^{1/2}.$$

When  $\delta\nu_{HB} > \Delta\nu_{MDR}$ , it can be shown that integration of the expression for  $\eta$  results in no lifetime change. However, in the intermediate regime,  $\Delta\nu_{MDR} > \delta\nu_{HB} > \delta\nu_{MDR}$ , the ratio  $\eta$  simply reduces to approximately  $\Delta\nu_{MDR} / \delta\nu_{HB}$ . A 14- $\mu\text{m}$ -diam alcohol ( $m = 1.36$ ) droplet, for example, has  $\Delta\nu_{MDR} \approx 150 \text{ cm}^{-1}$  and so species with  $\delta\nu_{HB} < 150 \text{ cm}^{-1}$  could exhibit lifetime changes through cavity QED effects. Note that in the intermediate regime, the enhancement is not dependent on cavity  $Q$  as suggested by Purcell's formula. Each MDR that satisfies the condition  $\delta\nu_{HB} > \delta\nu_{MDR}$  contributes equally [9] to the integral since the product of spectral width ( $\propto 1/Q$ ) and peak mode density per frequency ( $\propto Q$ ) is constant. In our experiment, we selected an emission species, chelated-europium ions, with a narrow homogeneous width (approximately  $50 \text{ cm}^{-1}$ ) and a droplet size sufficiently small (approximately  $10 \mu\text{m}$  diam and  $\Delta\nu_{MDR} \approx 200 \text{ cm}^{-1}$ ) to observe QED effects.

A vibrating orifice aerosol generator (VOAG) [17] was used to produce a falling linear stream of nearly identical 10- to 24- $\mu\text{m}$ -diam,  $10^{-2}\text{-M}$  tetrakis form of europium benzoyltrifluoroacetate  $[\text{Eu}(\text{BTF})_4\text{P}]$  in dimethylformamide-ethanol-methanol (DMFA) solution [20] droplets which were excited by a 457-nm cw argon-ion laser (see Fig. 2). The sample liquid, cooled to  $-8^\circ\text{C}$  to maximize quantum efficiency and to prevent droplet downstream evaporation, is direct pressure fed to either a 5- or 10- $\mu\text{m}$  vibrating orifice. The droplet stream was calibrated by inducing a size ramp by sweeping the frequency synthesizer used to drive a piezoelectric transducer mounted on the orifice. By comparing the experimental elastic-scattering size spectra obtained using a 632.8-nm He-Ne laser to spectra calculated from Lorenz-Mie theory, the size and index of refraction of the droplet could be obtained as previously described [16,17]. Droplets were constant in size to 2 parts in  $10^5$  at each point in the stream and to better than 1 part in  $10^3$  over the 1-cm fall distance.

The excitation beam was focused to a 30- $\mu\text{m}$ -diam spot illuminating approximately one droplet at a time. We tuned the particle stream diameter by varying the VOAG

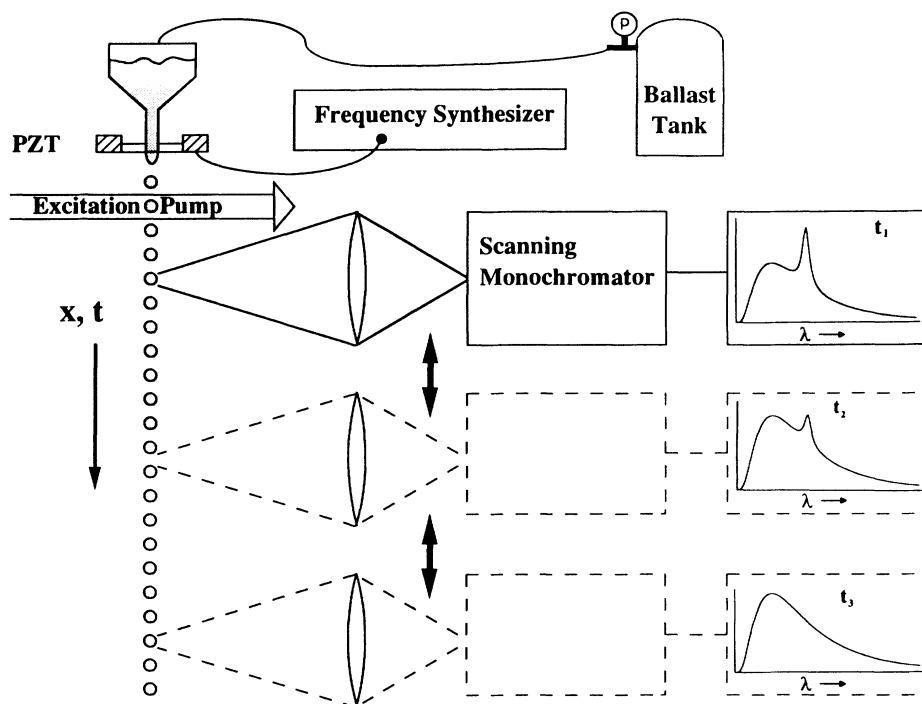


FIG. 2. Experimental schematic of the apparatus used in the droplet emission studies.

frequency until the droplets were in optical resonance with the excitation laser. The resonance condition was maintained during data collection and created an excited  $\text{Eu}^{+3}$  population spatially concentrated near the droplet rim as previously described. Droplet emission was observed using a 1-m Spex double spectrometer and cooled photomultiplier with photon-counting electronics. The spectral region from 610 to 625 nm was examined. By imaging the droplets at various distances from the point of excitation as they fall, the particle stream was converted into a mechanical framing camera (see Fig. 2) and the temporal evolution of the europium ion spectral emission is sequentially mapped. Droplets further downstream correspond to successively later times after excitation (1 mm  $\approx$  0.1 ms). Because the stream velocity slows as the droplets fell depending on the particle diameter, we calibrated the precise distance versus time dependence for each droplet size by first nonresonantly exciting the particles using a 20-ns, 355-nm light pulse and measuring the delay time that emission was first observed further downstream. After calibration, the spectral time histories shown in Figs. 3 and 4, were obtained using the cw 457-nm excitation source to resonantly excite the stream. Each time frame was obtained by imaging the emission from three neighboring downstream droplets onto the slits of a scanning monochromator and collecting a spectrum. Successive frames were obtained by vertically translating the collection lens and repeating this procedure.

Figures 3 and 4 show successive time frames of the  $\text{Eu}(\text{BTF})_4\text{P}$  emission spectrum ( $^5D_0$  to  $^7F_2$  transition) for nominally 24- and 10- $\mu\text{m}$ -diam droplets, respectively. The 24- $\mu\text{m}$  data ( $\Delta\nu_{\text{MDR}} \approx \delta\nu_{\text{HB}}$ ) may be considered a

control experiment that is expected to yield an observed lifetime close to that of free space europium ions. Indeed, the observations of Fig. 3 are consistent with this expectation. The experimental ratio of MDR peak heights to

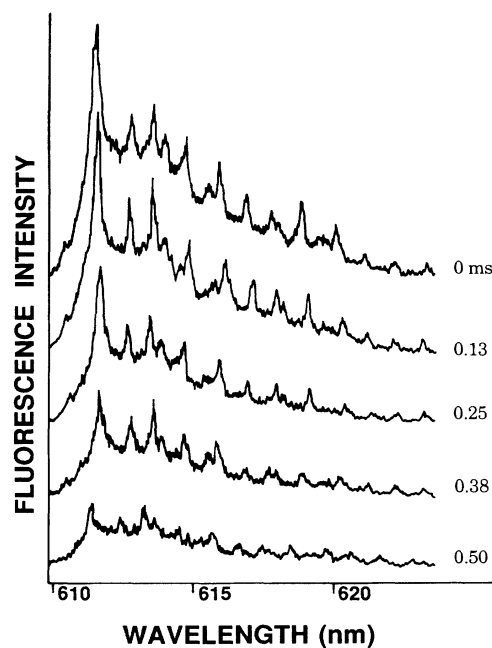


FIG. 3. Successive time frames show europium ion emission spectra from resonantly pumped control 24- $\mu\text{m}$ -diam dimethylformamide-alcohol solution droplets. Here, the lifetimes of the MDR peaks as well as that of the broad non-resonant emission are nearly equal to the free-space europium lifetime.

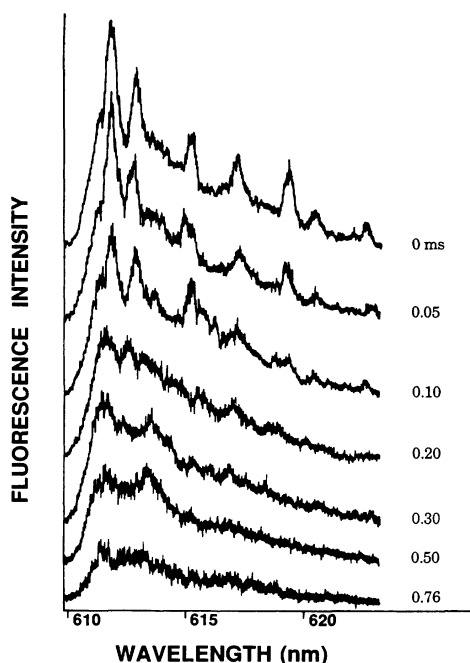


FIG. 4. Successive time frames showing europium ion emission spectra from resonantly pumped 10- $\mu$ m-diam DMFA solution droplets. Here, the MDR features decay more quickly ( $2.5\times$ ) and the broad inhibited background more slowly ( $1.5\times$ ) than free-space europium ion excitation.

that of the nonresonant broadband emission remains constant with time and both display  $1/e$  amplitude decays of about 0.5 msec, close to the free-space europium-ion lifetime. Even though the lifetime is not altered, the presence of MDR emission peaks illustrates that the cavity continues to induce significant spectral changes (i.e., the emission rates per unit frequency on- and off-resonance remain markedly different) even in large droplets. Shown are several orders of MDR's having  $Q$ 's ranging from  $10^4$  to  $10^8$ . The emission at each instant is proportional to the population of the upper state which decays at a rate determined by the averaging effect of simultaneous transitions to both enhanced and inhibited states over the homogeneous linewidth and so, in this case, does not appreciably change. In Fig. 4, however,  $\Delta\nu_{\text{MDR}}/\delta\nu_{\text{HB}}$  is increased to about 4 by reducing the droplet size. The MDR emission features in this case are observed to decay in less than 0.2 ms. In addition, the broadband emission that presumably emanates from rim inhibited locations

has a measurable  $1/e$  lifetime of 0.76 ms, approximately 50% longer than the free-space value.

The 0.5-ms curve of Fig. 4, absent of MDR features, resembles the characteristic bulk emission spectrum. The peaks at 611.5 and 613 nm are lines (not MDR's) associated with the tetrakis form of chelated europium ion having a common  $^5D_0$  upper state and a  $^7F_2$  lower state that is split by interaction with the chelates. Each line is about 2 nm wide. Note that with regard to QED enhancement, the homogeneous width of a single line is the relevant parameter. The broad emission from 614 to 620 nm consists of several lines due to the tris species which is also formed during the tetrakis synthesis. It is interesting that this species also shows significant lifetime shortening and lengthening due to cavity effects.

The experimental observations shown in Fig. 4 cannot be explained by noncavity QED phenomena. The excitation intensity was kept at a level low enough to ensure the absence of lasing while the particle was in the excitation beam. When the droplet moves out of the excitation beam, any stimulated emission that may have been present must be cavity dumped on time scales of the order of the cavity lifetime (approximately 1 ns) and could not possibly play a role in down-stream lifetime measurements that were typically five orders of magnitude longer. One can also rule out apparent MDR emission decay due to the excited-state population migrating out of the modal volume. Droplets in this size range have Sherwood numbers that are much less than 1 and so internal molecular transport should be dominated [21] by diffusion rather than convective flow. A calculation of the characteristic diffusion time peculiar to the modal spatial geometry indicates a value several orders of magnitude longer than the time scale of this experiment. In addition, diffusive population loss would have displayed a  $t^{-1/2}$  decay dependence not supported by the data. The absence of a short MDR lifetime in the control observations for larger droplets lends strong experimental support to these conclusions.

In summary, we have made the first direct observation of lifetime shortening ( $>2.5\times$ ) and lengthening ( $>1.5\times$ ) due to the effects of cavity QED of a fluorophore in a naturally formed droplet microcavity. This effect on lifetime depends principally on ratio of the spectral spacing of MDR's of the same order to that of the homogeneous linewidth of the emitting species and is expected to be independent of cavity  $Q$  when  $\delta\nu_{\text{HB}} > \delta\nu_{\text{MDR}}$ .

This work was supported by the Office of Naval Research.

\*Also at Potomac Photonics Inc., Lanham, MD 20706.

- [1] E. M. Purcell, Phys. Rev. **69**, 681 (1946).
- [2] P. Stehle, Phys. Rev. A **2**, 102 (1973).
- [3] P. Goy, J. M. Raimond, M. Gross, and S. Haroche, Phys. Rev. Lett. **50**, 1903 (1983).
- [4] D. Kleppner, Phys. Rev. Lett. **47**, 233 (1981).
- [5] R. G. Hulet, E. S. Hilfer, and D. Kleppner, Phys. Rev.

Lett. **55**, 2137 (1985).

- [6] F. De Martini, G. Innocenti, G. Jacobovitz, and P. Mataloni, Phys. Rev. Lett. **59**, 2955 (1987); F. De Martini and G. Jacobovitz, *ibid.* **60**, 1711 (1989); F. De Martini, M. Marrocco, P. Mataloni, and L. Crescentini, Phys. Rev. A **43**, 2480 (1991).
- [7] H. Yokoyama, K. Nishi, T. Anan, H. Yamada, S. D. Bror-

- son, and E. P. Ippen, *Appl. Phys. Lett.* **57**, 2814 (1990); M. Suzuki, H. Yokayma, S. D. Brorson, and E. P. Ippen, *ibid.* **58**, 998 (1991).
- [8] D. J. Heinzen, J. J. Childs, J. E. Thomas, and M. S. Feld, *Phys. Rev. Lett.* **58**, 1320 (1987).
- [9] S. C. Ching, H. M. Lai, and K. Young, *J. Opt. Soc. Am. B* **4**, 1995 (1987); **4**, 2004 (1987).
- [10] S. C. Hill and R. E. Benner, *J. Opt. Soc. Am. B* **3**, 1509 (1986).
- [11] R. E. Benner, P. W. Barber, J. F. Owen, and R. K. Chang, *Phys. Rev. Lett.* **44**, 475 (1980).
- [12] J. F. Owen, P. W. Barber, P. B. Dorain, and R. K. Chang, *Phys. Rev. Lett.* **47**, 1075 (1981).
- [13] H. Chew, *Phys. Rev. A* **38**, 3410 (1988); **37**, 4107 (1988); *J. Chem. Phys.* **87**, 1355 (1987).
- [14] H. M. Lai, P. T. Leung, and K. Young, *Phys. Rev. A* **37**, 1597 (1988).
- [15] A. J. Campillo, J. D. Eversole, and H.-B. Lin, *Phys. Rev. Lett.* **67**, 437 (1991).
- [16] J. D. Eversole, H.-B. Lin, and A. J. Campillo, *Appl. Opt.* (to be published); H.-B. Lin, A. L. Huston, J. D. Eversole, and A. J. Campillo, *J. Opt. Soc. Am. B* **7**, 2079 (1990).
- [17] H.-B. Lin, J. D. Eversole, and A. J. Campillo, *Rev. Sci. Instrum.* **61**, 1018 (1990).
- [18] H. Yokoyama and S. D. Brorson, *J. Appl. Phys.* **66**, 4801 (1989).
- [19] P. Chylek, *J. Opt. Soc. Am.* **66**, 285 (1976).
- [20] C. Brecher, H. Samelson, and A. Lempicki, *J. Chem. Phys.* **42**, 1081 (1965).
- [21] R. Clift, J. R. Grace, and M. E. Weber, *Bubbles, Drops and Particles* (Academic, New York, 1972).

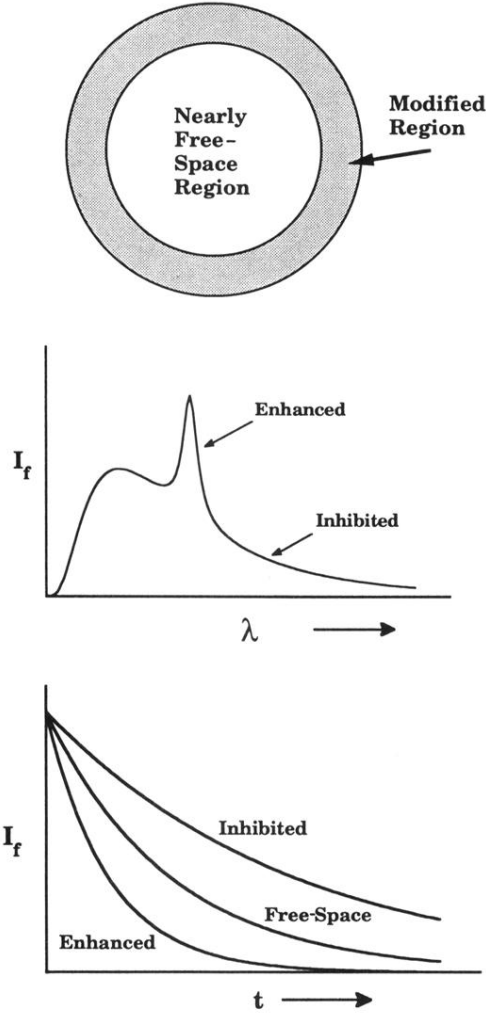


FIG. 1. Outline of the experimental approach. When the droplet is in optical resonance with the exciting laser, an excited-state europium ion population is created near the droplet-air interface (top, shaded region). Within this region, emission rates are modified and spectra appear as illustrated in the middle of the figure. The broad off-resonant spectral components resemble the free-space spectrum, but emanate from inhibited spatial locales and decay more slowly (see bottom). The resonant emission rate is enhanced, leading to the formation of a spectral peak which decays more rapidly than the usual free-space rate. The emission from the droplet rim is an admixture of components displaying both inhibited and enhanced lifetimes.

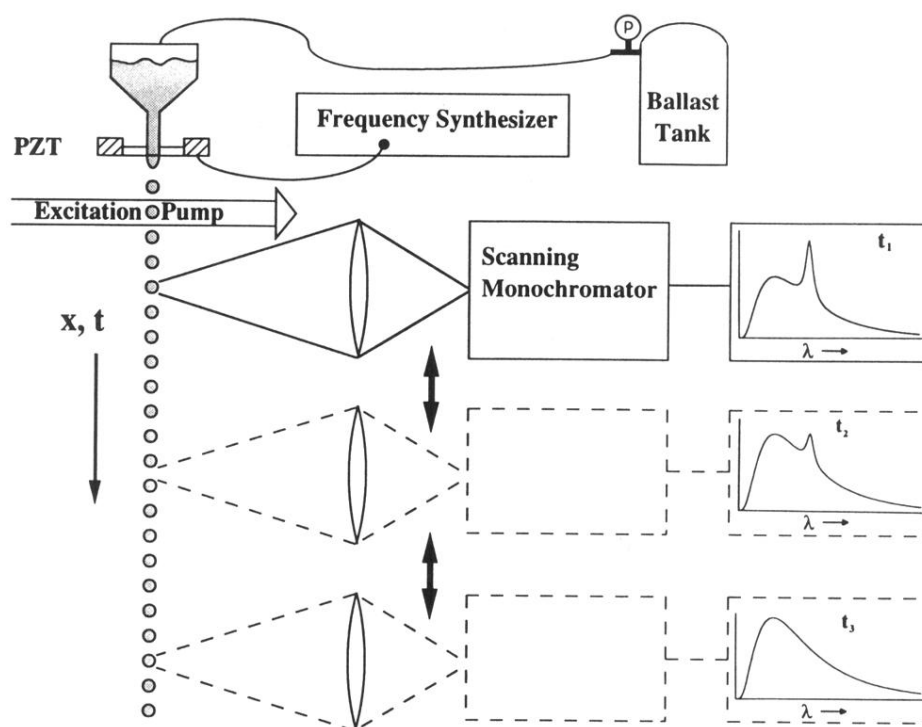


FIG. 2. Experimental schematic of the apparatus used in the droplet emission studies.